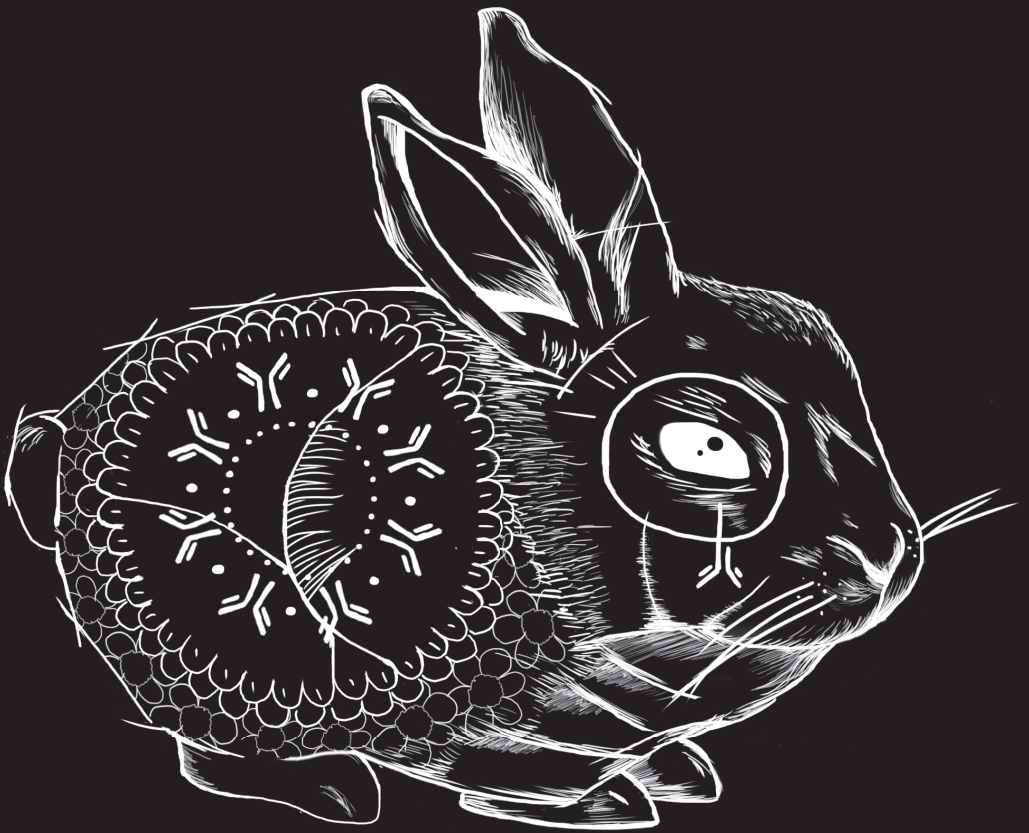Cover Page

The handle http://hdl.handle.net/1887/46717 holds various files of this Leiden University dissertation.
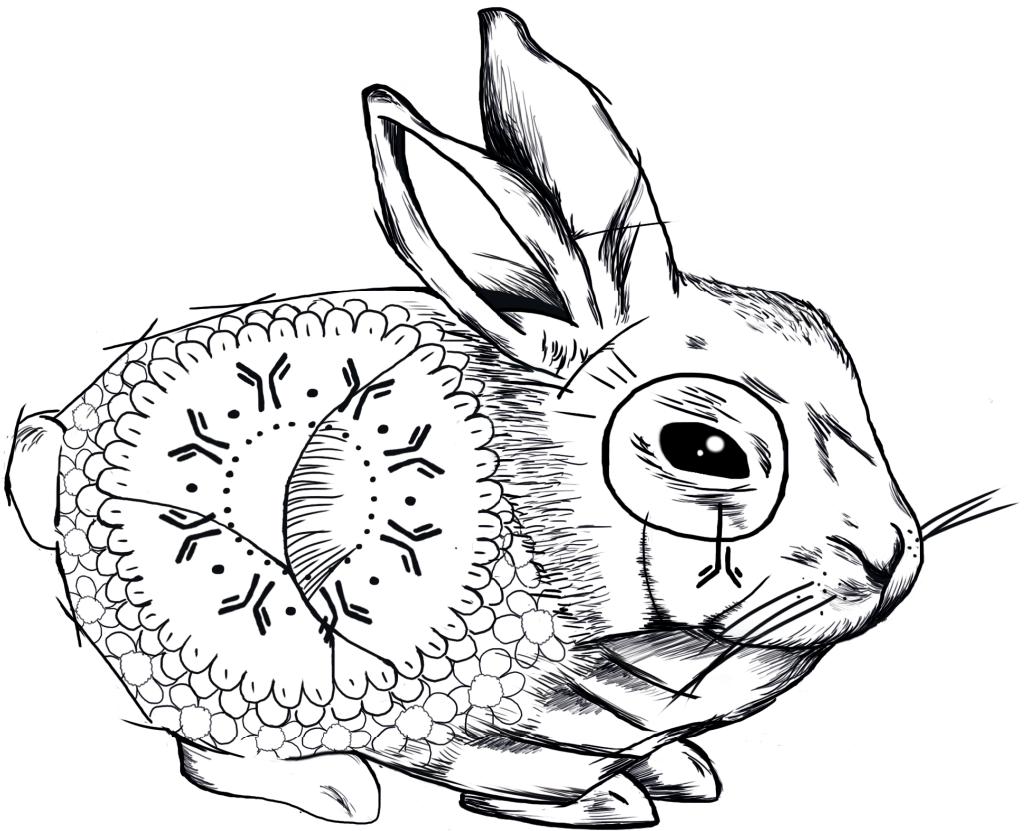
Author: Admiraal, R.
Title: Individualized dosing of serotherapy in allogeneic hematopoietic cell transplantation - a delicate balance
Issue Date: 2017-03-15

PART II

Pharmacokinetics of Serotherapy

Chapter 3

Population Pharmacokinetic Modeling of Thymoglobulin in Children Receiving Allogeneic-Hematopoietic Cell Transplantation:
Towards Improved Survival Through Individualized Dosing

Rick Admiraal

Charlotte van Kesteren

Cornelia M Jol-van der Zijde

Maarten J.D. van Tol

Imke H. Bartelink

Robbert G.M. Bredius

Jaap J. Boelens

Catherijne A.J. Knibbe

ABSTRACT

Background and Objectives

To prevent graft-versus-host disease and rejection in hematopoietic cell transplantation (HCT), children receive Thymoglobulin®, a polyclonal antibody acting mainly by depleting T cells. The therapeutic window is critical as over-exposure may result in delayed immune reconstitution of donor T cells. In this study, we describe the population pharmacokinetics of Thymoglobulin® as a first step towards an evidence-based dosing regimen of Thymoglobulin® in pediatric HCT.

Methods

Serum active Thymoglobulin® concentrations were measured in all pediatric HCTs performed between 2004 and 2012 in two pediatric HCT centers in The Netherlands. Population pharmacokinetic analysis was performed using NONMEM® version 7.2.

Results

A total of 3,113 concentration samples from 280 pediatric HCTs were analyzed, with age ranging from 3 months to 23 years old. The cumulative Thymoglobulin® dose was 10 mg/kg in 94% of the patients given in 4 consecutive days. A model incorporating parallel linear and concentration-dependent clearance of Thymoglobulin® was identified. Body weight [for linear clearance (CL) and central volume of distribution] as well as lymphocyte counts pre-Thymoglobulin® infusion (for CL) were important covariates. As such, the current dosing regimen results in higher exposure in children with a higher bodyweight and/ or a lower lymphocyte count pre-Thymoglobulin® infusion.

Conclusion

This model can be used to develop an individual dosing regimen for Thymoglobulin®, based on both body weight and lymphocyte counts, once the therapeutic window has been determined. This individualized regimen may contribute to a better immune reconstitution and thus outcome of allogeneic HCT.

INTRODUCTION

Since the 1970s, anti-thymocyte globulin (ATG) has been widely applied as serotherapy in order to prevent acute graft-versus-host disease (GvHD) and graft rejection in patients undergoing non-HLA-identical hematopoietic cell transplantations (HCTs)[1–4]. The introduction of ATG to the conditioning regimen has indeed led to a significant decrease in severe acute and chronic GvHD[5,6]. How- ever, too high doses of ATG impair the required immune reconstitution after HCT. As such, there is a delicate balance between prevention of GvHD on one side and the promotion of immune reconstitution on the other.

Theoretically, the incidence of GvHD or rejection versus delayed immune reconstitution may result from a variable exposure of ATG. Prolonged and/or high exposure to ATG leading to lymphodepletion with delayed or absent immune reconstitution may result in relapse of the malignancy or viral infections, while a short or absent ATG- related lymphodepletion may result in limited or no protection against acute GvHD[7,8]. During the first weeks to months after transplantation, T cell reconstitution depends on peripheral expansion, the division of mature T cells infused with the graft. Hereafter, depending on the thymus function, definitive repopulation of the T cells will take place through thymopoiesis[9–11]. As peripheral expansion is restricted by circulating ATG, excess ATG due to relative overdosing leads to delayed or even absent reconstitution of T cells, possibly resulting in lethal viral reactivations and relapse[12,13].

Thymoglobulin® is the most commonly used preparation of ATG in pediatric HCT. Children usually receive an empirically derived cumulative Thymoglobulin® dose of 10 mg/kg, given in 4 days, starting 4–6 days before transplantation. Thymoglobulin® is not registered in pediatrics, and as such its use is off-label. Particularly in children, the pharmacokinetics of a drug may differ as a result of changes in body composition and maturation in organ function[14]. This variability in pharmacokinetics influences drug exposure, which in turn determines the drug response of pharmacodynamics. In order to maintain efficacy while reducing adverse effects of drugs across the entire pediatric age range, identification of the pharmacokinetic/ pharmacodynamic relationships and the effect of growth and maturation on the different pharmacokinetic and pharmacodynamic parameters involved are crucial[15–17]. This has been shown before in pediatric HCT, where individualized busulfan dosing has led to a significant decrease in toxicity whilst remaining effective in terms of relapse and engraftment[18,19].

To date, only a limited number of papers on the pharmacokinetics of ATG (Thymoglobulin® and other preparations) have been published, with very few in children[20–26]. The half-life of Thymoglobulin® is reported to be 7–14 days[20,26]. The available evidence for Thymo-

globulin® shows that pharmacokinetics change during childhood, with varying exposures possibly leading to different outcomes[25,26]. Therefore, the aim of this study was to develop a population pharmacokinetic model for active Thymoglobulin® as a first step in describing Thymoglobulin® pharmacokinetics/ pharmacodynamics and thus developing a basis for an individualized dosing regimen. The focus was on active Thymoglobulin®, which is the fraction that is directed against human targets and that can be held responsible for its pharmacological action in humans[27]. Since Thymoglobulin® pharmacokinetics are pivotal both in preventing acute GvHD and rejection as well as assuring a successful and timely immune reconstitution, individualizing the dosing may improve survival in pediatric HCT.

METHODS

Study Design and Patients

For this pharmacokinetic analysis, all patients receiving an HCT between April 2004 and December 2012 with Thymoglobulin® as part of the conditioning in the pediatric hematopoietic stem cell transplantation programs of the University Medical Center Utrecht (UMCU) and the Lei- den University Medical Center (LUMC), The Netherlands, were included. In case of multiple transplants in one patient, concentrations of Thymoglobulin® in all transplants were included, provided no serotherapy (i.e., ATG, alemtuzumab) was given in the last 3 months before second/third transplantation. Patients receiving serotherapy other than Thymoglobulin® within a period of 3 months before HCT were excluded. Informed consent was given by the child and/or the parents (the former when over 12 years old). All data were collected after written informed consent was obtained in accordance with the Declaration of Helsinki and institutional ethical committee approval for sample and data collection, trial numbers METC 05/143 and METC 11/063-k (UMCU) and P01.028 (LUMC).

Patient characteristics including transplantation details of the studied patients are shown in Table 1. Patients typically received Thymoglobulin® over 4 h in a cumulative dose of 10 mg/kg divided over 4 consecutive days starting 5 days before HCT. At the discretion of the treating team of physicians, some patients received a lower dose of Thymoglobulin® (7.5 mg/kg) and/or received Thymoglobulin® earlier (day –9). Some patients with hemophagocytic lymphohistiocytosis received a higher dose of up to 20 mg/kg. Pharmacokinetic samples were avail- able in the elimination phase of Thymoglobulin® in all patients, whilst in patients treated in the LUMC, peak and trough concentrations (collected 15 min after and 15 min before 4-h infusion, respectively) were also available, which in light of the very long half-life can be seen as the true peak and trough concentrations. Generally, samples were taken weekly (Mondays/Thursdays in UMCU, Monday/Wednesday/Friday in LUMC) until 12 weeks after transplantation. Collected samples were centrifuged upon drawing; plasma was

Characteristics	Leiden	Utrecht	Total
Number of patients (n)	153	114	267
Number of HCTs (n)	159	121	280
Male sex (%)	67	57	62
Age (years)	6.5 (0.4-19)	5.9 (0.2-23)	6.5 (0.2-23)
Actual body weight (kg)	21 (4.7-75)	20 (3.7-96)	21 (3.7-96)
BSA (m^2)	0.84 (0.28-1.95)	0.82 (0.14-2.1)	0.83 (0.14-2.1)
Number of samples [n (mean per patient)]	2352 (15)	761 (6)	3113 (11)
Starting day Thymoglobulin® (days before transplantation)	5 (3-15)	5 (1-19)	5 (1-19)
Lymfocyte count at first dose Thymoglobulin® (x 10^9)	0.1 (0.01-4.5)	0.71 (0.01-10.4)	0.29 (0.01-10.4)
Cumulative Thymoglobulin® dose (%) <9 mg/kg	3	5	4
9-11 mg/kg	97	89	94
>11 mg/kg	0	6	2
Diagnosis (%)			
Malignancy	50	42	47
Immune deficiency	16	24	19
Bone marrow failure	4	10	6
Metabolic disease	0	21	9
Benign hematology	30	1	18
Auto-immune disease	0	2	1
Stem cell source (%)			
Bone marrow	63	29	49
Peripheral blood stem cells	23	5	15
Cordblood	14	60	34
Cordblood plus haplo or 2nd cordblood	0	6	2
Conditioning regimen (%)			
Reduced intensity	0	7	4
Chemotherapy-based	72	78	74
TBI-based	28	15	22

Table 1. Patient characteristics. Values are shown as median (range) unless otherwise specified. BSA: body surface area, TBI: total body irradiation

stored to be analyzed in batches. Conditioning regimens were given according to (inter) national protocols. Gut decontamination and infection prophylaxis were given according to local protocols. Patients were treated in high-efficiency, particle-free, air-filtered, positive-pressure isolation rooms. Patients received clemastine combined with either di-adreson-F aquosum (2 mg/ kg) or prednisolone (2 mg/kg) before and during Thymoglobulin® infusion.

Measurement of Active Thymoglobulin® and Anti-Thymoglobulin® Antibodies

Active Thymoglobulin®, defined as Thymoglobulin® capable of binding to HUT-78 cells, was measured using a quantitative flow cytometry assay[25], based on a method described

by Rebello[28]. In short, HUT-78 T cells (PHACC, Porton Down, UK) were incubated with fourfold dilutions of patient serum, followed by washing and incubation with Alexa Fluor 647 labeled with goat anti-rabbit IgG (Biosource, Life Invitrogen, Carlsbad, CA, USA). To prepare standards with predefined active Thymoglobulin® concentrations, Thymoglobulin® was serially diluted two- fold in triplicate to produce a range of Thymoglobulin® standards ranging from 5 to 0.005 AU/mL. Active Thymoglobulin® is expressed in arbitrary units (AU): Thymoglobulin® 5 mg/mL is arbitrarily set to contain a concentration of 5,000 AU/mL of active Thymoglobulin®. The lower limit of quantification was 0.01 AU/mL. Cells were washed and analyzed by flow cytometry on a FACS scan (Becton Dickinson Biosciences, Franklin Lakes, NJ, USA); mean fluorescence intensities of standard dilutions were plotted against the active Thymoglobulin® concentrations and the reference curve was used to determine the concentration of active Thymoglobulin® in patient samples. Samples were tested in duplicate with an accepted coefficient of variation of 0.2, both in high and low ranges.

Anti-Thymoglobulin® antibodies in classes IgA, IgM, and IgG were measured using an ELISA. After blocking, patient sera were applied to Thymoglobulin®-coated plates. Anti-ATG antibodies were detected using alkaline phosphatase-conjugated rabbit-anti-human (IgG; Jackson ImmunoResearch Europe, Newmarket, UK) or goat-anti- human (IgM, IgA; Jackson) antibodies[25], adsorbed for rabbit IgG. As literature shows IgG anti-ATG antibodies to significantly influence Thymoglobulin® pharmacokinetics[25], samples with IgG anti-Thymoglobulin® antibodies were marked. While the decline in concentration after occurrence of these antibodies was variable, these samples (n = 13 from six patients) were excluded from the analysis.

Population Pharmacokinetic Analysis

To allow analysis of sparse and unbalanced data, the population approach was applied for pharmacokinetic modeling[15,16]. This method uses data from all patients simultaneously to estimate pharmacokinetic parameters for individual patients as well as the whole cohort. For this purpose, the non-linear mixed effects modeling software NONMEM version 7.2 (Icon, Hanover, MD, USA)[29] was used, with Pirana version 2.8.1[30] and R version 3.0.1[31] for visualization of data. The estimation method used was first-order conditional estimation with interaction (FOCE-I). Active Thymoglobulin® concentrations measured as AU/mL, were logarithmically transformed, and fitted simultaneously. Observations below limit of quantification (BLQ) were set at half the limit of quantification, with following samples being deleted[32]. Other methods for handling BLQ were investigated (M3 and removal of BLQ[32]); this did not result in an improvement of the model. Modeling of data was performed in four steps: (1) selection of a structural and statistical model; (2) selection of an error model; (3) covariate analysis and selection; and (4) internal validation of the model. Individual

pharmacokinetic parameters (post hocs) such as clearance of the individual patient were estimated using the POSTHOC option in NONMEM, according to Eq. 1:

$$P_i = P_{pop} \cdot e^{\eta_i} \qquad \text{(Eq. 1)}$$

where P_i is the individual or post hoc value of the parameter in the ith individual, P_{pop} the population value for that parameter, and η_i the inter-individual variability of the *i*th person samples from a distribution with a mean zero and variance of ω^2 with a log-normal distribution.

A proportional error model was used, so that for the *j*th observation in the *i*th individual, the observations are described using Eq. 2:

$$Y_{i,j} = C_{pred,i,j} \cdot (1 + \epsilon) \qquad \text{(Eq 2)}$$

where $Y_{i,j}$ is the observed concentration, $C_{pred,i,j}$ is the predicted concentration for *j*th observation in the ith individual, and ϵ is the error samples from a distribution with a mean zero and variance of σ^2.

In the model-building process, several criteria were applied. A decrease in objective function value (OFV) over 3.84 points between two hierarchical (sub) models was considered statistically significant; this correlates with $p<0.05$ based on a Chi-squared (χ^2) distribution for 1 degree of freedom. In addition, goodness-of-fit plots [observed vs. both individual and population predictions of concentrations as well as conditional weighted residuals (CWRES) versus time and observed concentrations] were evaluated with emphasis on the population predictions. Furthermore, confidence intervals of parameter estimates, g-shrinkage, and visual improvement of the goodness-of-fit plots were used to evaluate the models. Inter-occasion variability on the different parameters was tested for the subsequent doses to assess changes in pharmacokinetic parameters between doses.

Covariate Selection

Possible covariates, including, among others, patient characteristics and disease- and treatment-related variables, were studied. Inter-individual variability as well as post hocs, weighted residuals (WRES) and CWRES were independently plotted against covariates to evaluate possible relationships. While categorical covariates such as sex and treatment center were tested as a fraction for each category, continuous covariates were tested in linear and power functions (Eqs. 3 and 4):

$$P_i = P_{pop} \cdot \left(\frac{Cov_i}{Cov_{median}}\right)^k \qquad \text{(Eq. 3)}$$

$$P_i = P_{pop} \cdot \left(1 + \left(\frac{Cov_i}{Cov_{median}}\right) \cdot l\right) \qquad \text{(Eq. 4)}$$

where P_i and Cov_i are the value for parameter and covariate for the ith individual, respectively, P_{pop} is the population mean for parameter P, and Cov_{median} is the standardized value of the covariate. In the power function, the scaling factor is depicted by k. For Eq. 4, l represents the slope of the linear function.

Covariate model building was analogous to structural model building. Potential variables were evaluated using forward inclusion and backward elimination with a level of significance of <0.005 (-7.9 points in OFV) and <0.001 (-10.8 points in OFV), respectively. In addition, inclusion of a covariate in the model had to result in a decline in unexplained inter-individual variability before it was included in the final model[33,34].

Model Evaluation

Since the model will be used for future dose selection, proper internal validation of the model is of utmost importance[35]. To assess the predictive properties of the developed model, the proposed model was internally validated using bootstrap techniques. Here, a new dataset is repeatedly created through resampling using the individuals in the original dataset. One thousand replicated datasets were run using the bootstrap option in Perl speaks NONMEM (PsN) version 3.5.3[36]. Medians as well as the 2.5th and 97.5th percentiles were compared with parameter values estimated using the original dataset to check for discrepancies.

Another validation technique used was normalized prediction distribution errors (NPDE), simulating the prediction discrepancies while taking into account the predictive distribution and the correlation between observations in the same individual. The R-package NPDE was used for normalized prediction of errors[37].

Model-Based Simulations

With the evaluated model, simulations were performed on the basis of the currently recommended dose in children a cumulative dose of 10 mg/kg given in 4 h infusions in 4 consecutive days (2.5 mg/kg/day)] to visualize concentration–time profiles in representative children based on body weight and baseline lymphocyte counts.

RESULTS

Patients and Data

Active Thymoglobulin® concentrations obtained from 267 patients undergoing 280 HCTs were included from the two study centers. A total of 3,113 concentration samples were available with a median of 11 samples (range 1–32) per patient. A total of 13 observations from six patients were excluded due to anti-Thymoglobulin® IgG antibodies. Patient characteristics, other than diagnosis (benign hematology versus inborn errors of metabolism) and stem cell source, were equally distributed between the two centers (Table 1).

Structural Pharmacokinetic Model

Active Thymoglobulin® pharmacokinetics could be well- described using a two-compartment model (Fig. 1), which yielded a good description of the data in all age groups (Fig. 2). A two-compartment model was superior over a one-compartment model for statistical reasons [decrease in OFV of 382 points (p<0.001)] and improvement of goodness-of-fit plots (data not shown). A three-compartment model was tested and proved to be unstable with inaccurate parameter estimates. A proportional residual error was incorporated; adding an additive error did not significantly improve the model.
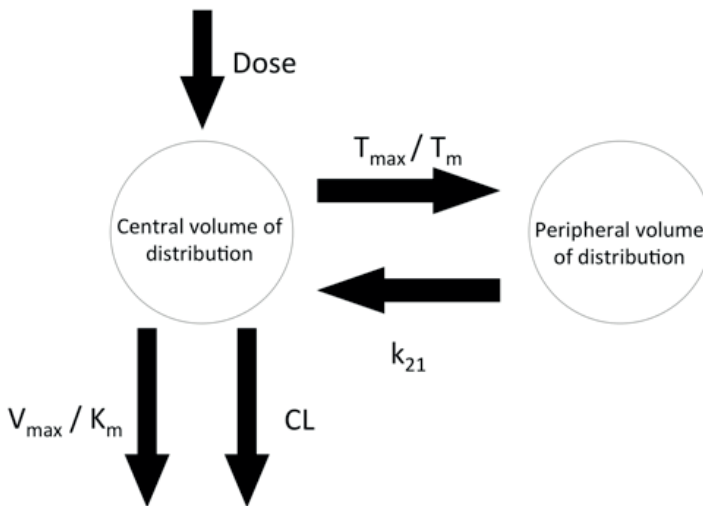

Figure 1. Model overview. Tmax: maximum rate of transport towards the peripheral compartment. Tm: concentration in central volume of distribution at 50% saturation of Tmax. K_{21}: rate of transport from the peripheral compartment to the central compartment. CL: linear clearance. V_{max}: maximum rate of elimination. K_m: concentration in central volume of distribution at 50% saturation of V_{max}.

Individual concentration–time plots indicated non-linear clearance, which was accounted for by a model with both linear clearance (CL) and saturable clearance, defined as the quotient of maximum elimination rate V_{max} and the Michaelis–Menten constant K_m (Fig. 1). This was previously described for antibody kinetics[38,39], and was found to lead to an improved description of the observations.

In addition, due to an under-prediction of concentrations during and shortly after the infusion, saturable distribution towards the peripheral compartment (T_{max}/T_m; Fig. 1) was included. This saturable distribution was parameterized as a coefficient of maximum transport rate (T_{max}) and the Michaelis–Menten constant (T_m). Figure 3 shows a structural

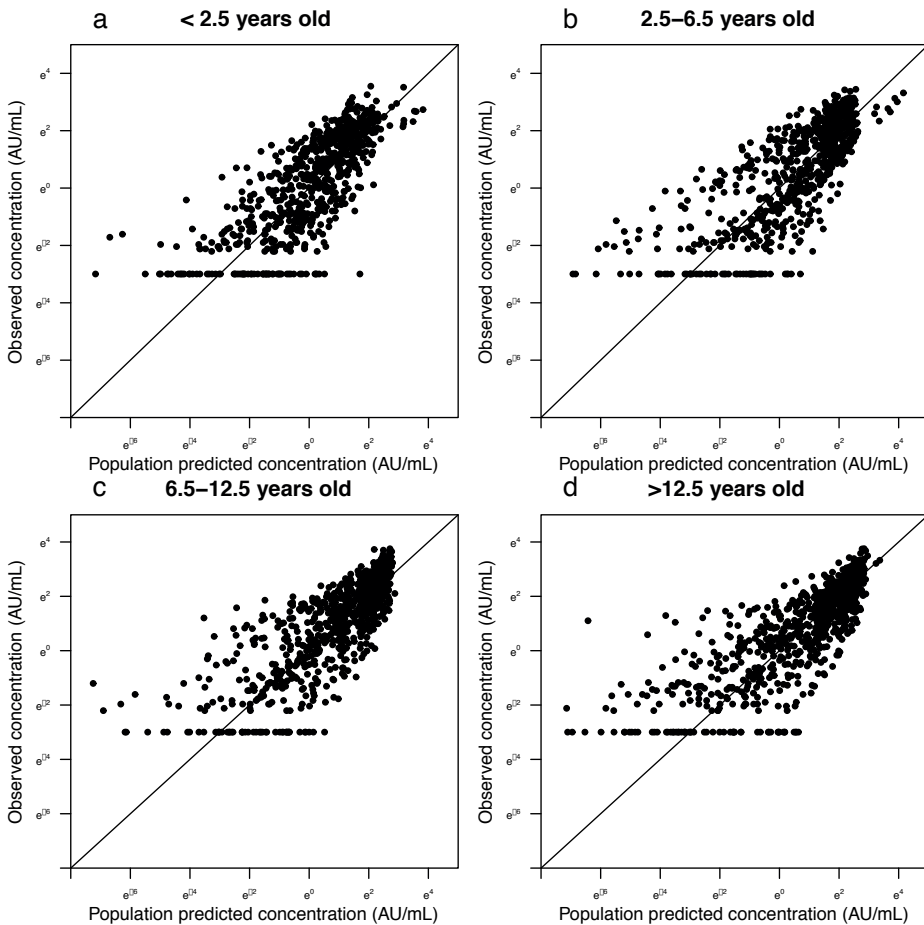Figure 2. Diagnostic plots of the final model: Observed versus population predicted active Thymoglobulin® concentrations split by quartiles of age. Panel a: <2.5 years, panel b: 2.5-6.5 years, panel c: 6.5-12.5 years, panel d: >12.5 years old. Dots: individual concentration versus population predicted value. Lines: x=y

under-prediction that can be seen at 3–7 days after start of Thymoglobulin® dosing (upper panel) and is corrected after inclusion of the saturable distribution (lower panel).

The addition of both of these non-linear functions to the final model as depicted in Fig. 1 led to a significant decrease in OFV [202 and 103 points (p<0.001), respectively] as well an improvement in goodness-of-fit plots. The Michaelis-Menten constants K_m and T_m were estimated in the observed concentrations range. Inter- occasion variability on CL and central volume of distribution (V_1) was tested for the subsequent doses; this yielded no significant improvement in model performance.
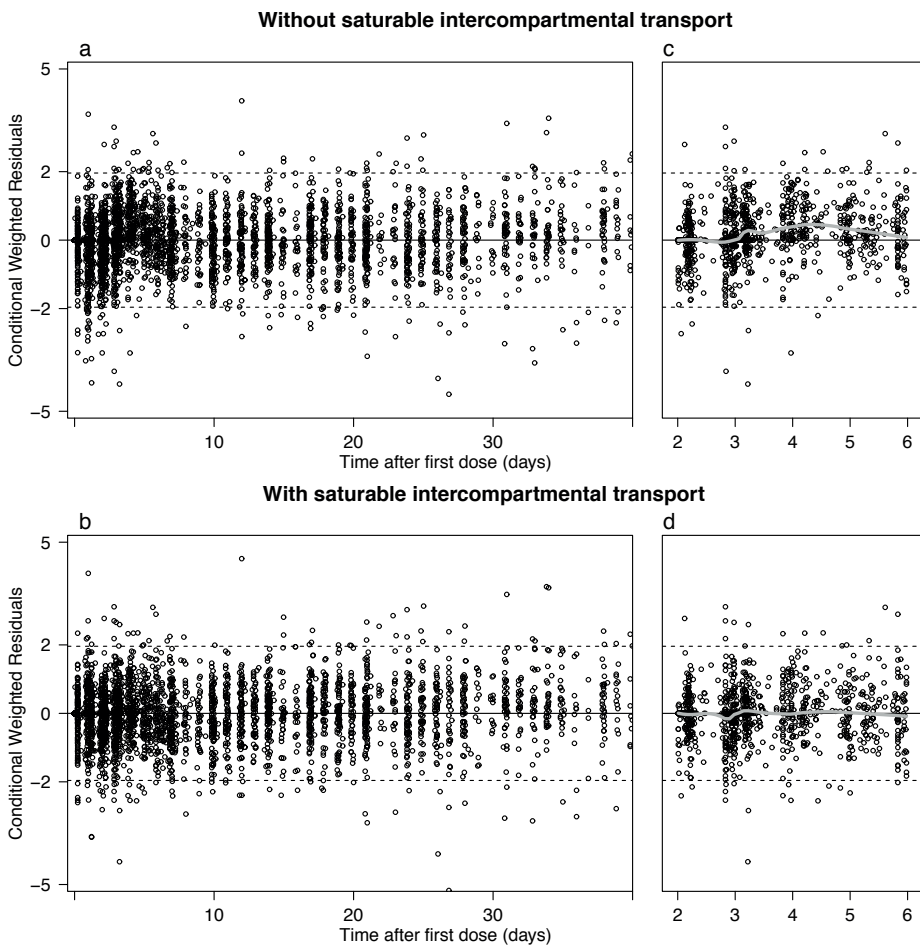

Figure 3. A trend in conditional weighted residuals (CWRES) versus time can be seen before introduction of saturable intercompartmental transport (panel a+b), which is accounted for after introduction (panel c+d). Panels a+c: all data; panels b+d: zoomed in to 2-6 days. Dots: CWRES per concentration sample, solid line CWRES=0, dashed lines ± 2SD, curved lines: spline regression.

Figure 4 shows how total clearance, defined as the sum of linear (CL) and saturable clearance (V_{max}/K_m) depends on the serum concentration of active Thymoglobulin®. At low concentrations, saturable clearance represents almost half of the total clearance. Above a certain concentration, the non-linear pathway becomes saturated, as seen in the decreasing saturable clearance. At concentrations above 10 AU/mL, the non-linear pathway is fully saturated, and total clearance is mostly dependent on the CL, with only a small contribution of the saturable clearance. From a clinical perspective, a concentration of 1 AU/mL is thought to be the lympholytic level in an in vitro setting[20].

			1000 bootstrap replicates (98% successful)	
	Dataset	Shrinkage	Median	2.5th-97.5th percentile
	[estimate (RSE)]	(%)		
Structural model				
$CL_i = CL_{pop} * \left(\dfrac{WT}{WT_{median}}\right)^k * \left(1 + \left(\dfrac{BL}{BL_{median}}\right) * l\right)$				
CL_{pop} (L/day)	2.2 (6%)		2.1	1.8-2.4
k	0.61 (13%)		0.62	0.45-0.80
l	0.12 (36%)		0.12	0.04-0.22
$V_{1,i} = V_{1,pop} * \left(\dfrac{WT}{WT_{median}}\right)^m$				
$V_{1,pop}$ (L)	7.8 (6%)		7.8	6.9-9.0
m	1.1 (7%)		1.1	0.92-1.3
$K_{21,pop}$	1.2 (18%)		1.2	0.79-1.8
$T_{max,pop}$ (AU/day)	156 (15%)		161	98-241
$T_{m,pop}$ (AU/L)	7.6 (21%)		7.5	4.9-13
$V_{max,pop}$ (AU/day)	1.8 (21%)		1.9	1.2-3.1
$K_{m,pop}$ (AU/L)	1.1 (21%)		1.1	0.67-1.8
Random variability				
Inter-individual variability on CL (%)	86 (5%)	5	85	76-94
Inter-individual variability on V_1 (%)	59 (7%)	20	58	49-67
Inter-individual variability on T_m (%)	106 (7%)	18	107	93-123
Inter-individual variability on V_{max} (%)	70 (12%)	54	70	49-93
Inter-individual variability on K_m (%)	177 (12%)	36	177	117-227
Proportional residual error (%)	32 (12%)	13	31	28-36

Table 2. parameter estimates and bootstrap results. WT: body weight (kg), WT_{median}: median population body weight (21 kg), BL: baseline (before first Thymoglobulin® infusion) lymphocyte count (x10^9 lymphocytes/L), BL_{median}: median baseline lymphocyte count (0.29 x 10^9 lymphocytes/L). CL: linear clearance; V_1: central volume of distribution, K_{21}: constant depicting distribution from the peripheral to the central compartment, T_{max}: maximum transport rate towards in saturable distribution towards peripheral compartment, T_m: Michaelis-Menten constant saturable distribution towards peripheral compartment, V_{max}: maximum transport rate for saturable clearance pathway, K_m: Michaelis-Menten constant saturable distribution for saturable clearance pathway.

Covariate Analysis

The covariate analysis showed actual body weight, body surface area (BSA, Mosteller formula) and age to influence CL and V_1, while lymphocyte count at first dose of Thymoglobulin® was a covariate on CL only. Actual body weight was the best predictor of CL and V_1 when compared with other body size parameters such as BSA and age, in terms of the decrease in OFV as well as improvement in goodness-of-fit plots. The decrease in OFV was 52 and 124 points, respectively ($p<0.001$). The relationship between bodyweight and both CL and V1 was best described by a power function (Eq. 3), with the exponent k being 0.61 in the relationship with CL, and 1.1 in the relationship with V_1. Lymphocyte count was tested as a covariate since it is a target for Thymoglobulin® mediating its clearance.

Lymphocyte counts were available both before chemotherapy and shortly before (1–4 h) the start of Thymoglobulin® infusion, which was after 1–2 days of chemotherapy. As the chemotherapy in the conditioning might be expected to cause a drop in the lymphocytes, both lymphocyte counts were evaluated. Both covariates were comparable in predicting
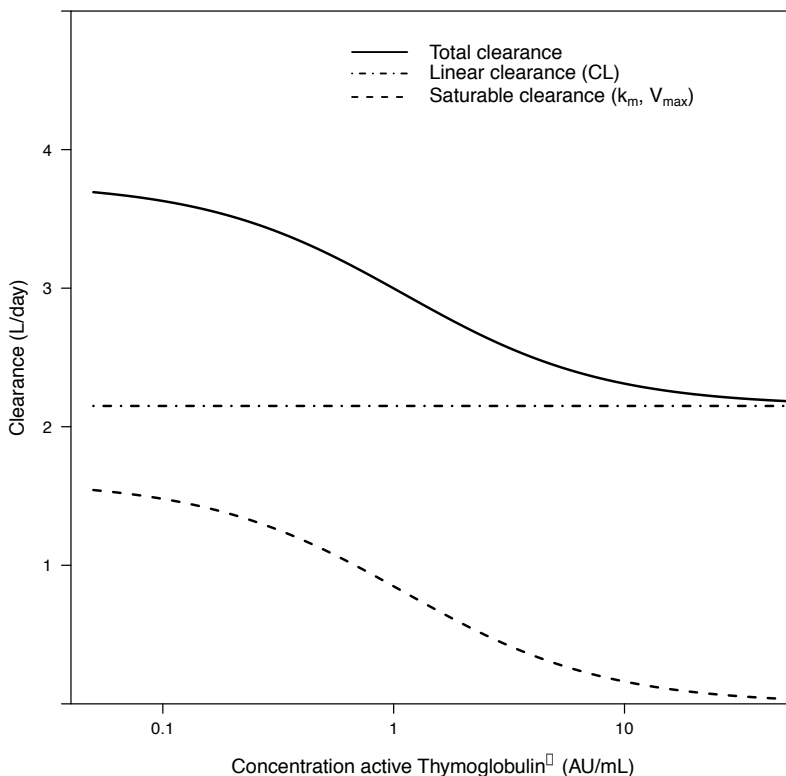

Figure 4. Total Thymoglobulin clearance, the sum of linear and saturable clearance, is dependent on active Thymoglobulin® concentrations.

inter-individual variability in CL. As the lymphocyte count before the first dose of Thymoglobulin® best reflects the current amount of available targets, this covariate was chosen. It was included as a linear relationship with CL (Eq. 4). Inclusion of this covariate led to a decrease in OFV of 54 points (p<0.001). As lymphocyte counts were not available after starting Thymoglobulin®, time was used as a surrogate for decreasing lymphocyte counts to take into account the decreasing lymphocyte counts after dosing of Thymoglobulin®. This did not result in an improvement of the model.

Diseases with a high peripheral lymphocyte burden were marked; these were no covariate on either clearance path- ways. No other covariates were identified, including treatment center, treatment year, and underlying disease.

Internal Validation of the Final Model

The final model with inclusion of all of the above-described covariates seemed stable in the bootstrap analysis with 98% successful runs. Median parameter values as well as the 2.5th and the 97.5th percentiles were in line with the model estimations and standard errors (Table 2). The NPDE showed a normal distribution of errors, with no trends in the NPDE versus time and NPDE versus predictions (Supplemental Figure 1).

Simulations

Figure 5 shows simulated Thymoglobulin® concentrations over time for patients with a body weight of 5, 20, and 40 kg, and lymphocyte counts at the first dose of Thymoglobulin® of 0,
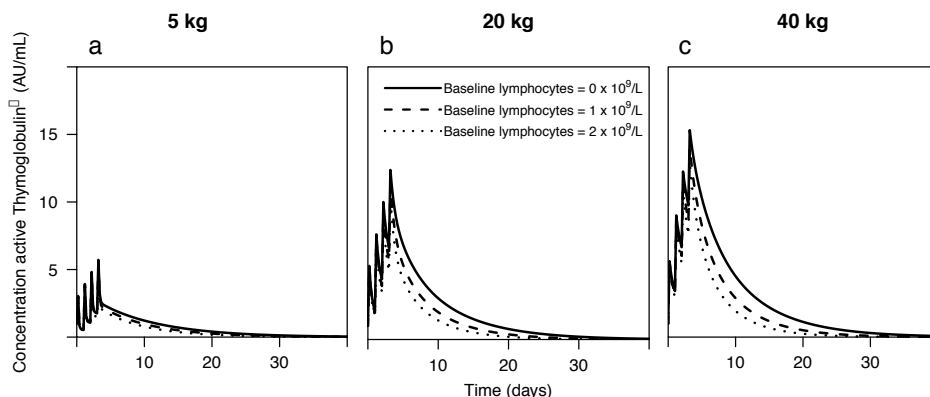

Figure 5. Model based simulation results of active Thymoglobulin® concentrations showing the population predictions of three representative individuals receiving Thymoglobulin® according to the current dosing regimen (cumulative dose of 10 mg/kg in 4 consecutive days), weighing 5 kg (panel a), 20 kg (panel b) and 40 kg (panel c). Solid lines: baseline lymphocytes 0x109/L, dashed lines: baseline lymphocytes 1x109/L, dotted lines: baseline lymphocytes 2x109/L.

1, and 2 x 10^9 cells/L, respectively, using the final model. The figure illustrates that, while using the currently approved dosing regimen, exposure increases with higher weight and/or lower baseline lymphocytes.

DISCUSSION

Thymoglobulin® is considered to play a pivotal role both in preventing GvHD and rejection as well as the occurrence of successful and timely immune reconstitution in HCT. We described the population pharmacokinetics of active Thymoglobulin® in a pediatric population.

Concentrations could be well predicted using this extensively validated model. Body weight and lymphocyte count at first dose of Thymoglobulin® proved to be predictors of CL and V_1. Simulation studies showed the current dosing regimen to be suboptimal, with patients with a higher body weight and/or a lower baseline lymphocyte count having a higher exposure.

In the proposed model, parallel linear and non-linear clearance was identified, which is frequently used for describing the pharmacokinetics of antibodies with non- soluble targets[38–40]. A true target-mediated drug disposition (TMDD) model was not possible due to the non-soluble targets, for which no concentrations were available, combined with the diversity of potential targets for Thymoglobulin® due to its polyclonal nature. This result is in line with the mechanism of action since active Thymoglobulin®, as all antibodies, is cleared through two mechanisms: target binding and non-specific degradation. Target binding is unique for the active fraction, whereas non-specific degradation occurs both in the active and the non-active fraction. The final model was developed based on the assumption that target binding is only possible when sufficient targets are available, resulting in a limited specific clearance in the case of a low number of targets. This also holds true for active Thymoglobulin®, although it has a great number of potential targets including T cells, B cells, natural killer cells, monocytes, and endothelium due to its manufacturing process in rabbits. To further unravel active Thymoglobulin® CL, the total Thymoglobulin® pharmacokinetics may be taken into consideration. Introducing information from total Thymoglobulin® pharmacokinetics, which is approximately 93% not reactive to human targets[27], more information may be gathered on non-active pharmacokinetics, which could sophisticate the current model.

The covariate model building showed actual body weight to be the best predictor for size on both CL and V_1. Lymphocyte count before the first dose of Thymoglobulin® proved to be a predictor for CL. Lymphocyte counts before conditioning (i.e., chemotherapy or

radiotherapy) as well as before the first dose of Thymoglobulin®, which were mostly just days apart, were available. Still, lymphocyte counts dropped between the two measurements in some patients, while other patients had a stable lymphocyte count. This effect appeared not to be related to the type of chemotherapy used. Nonetheless, pre-conditioning and pre-Thymoglobulin® lymphocyte counts were comparable predictors for inter-individual variability on CL. As pre- Thymoglobulin® lymphocyte counts best reflect the current amount of available targets, and therefore the potential for clearance through target binding, pre-Thymoglobulin® lymphocyte counts were used in the covariate model.

Several varieties of ATG are on the market: both horse (Atgam®, Pfizer, New York, NY, USA) and rabbit derived, with the latter being produced using human thymoid tissue (Thymoglobulin®, Sanofi (previously Genzyme), Lyon, France) or a Jurkat T cell leukemia line (ATG-Fresenius® S, Fresenius Biotech, Gräfelfing, Germany) as immunogen[5]. This pharmacokinetic model for Thymoglobulin® might to some extent reflect pharmacokinetics of other varieties of ATG, bearing in mind that the active fraction and its profile of specificities most likely differ[41]. For these products, in analogy to Thymoglobulin®, a population pharmacokinetic model should be developed, which could be partly based on this model.

One pediatric study has been published on the population pharmacokinetics of active Thymoglobulin® in HCT[26]. This study was performed in a relatively small cohort of 13 children, fitted using a two-compartment model with linear pharmacokinetics, where body weight was a covariate for both CL and V_1. Only the mean population value for CL was given, which is roughly in line with our results, although no parallel clearance was incorporated making interpretation difficult. No internal or external validation was performed in that study. Some other studies have been performed in children[21,25], adults[20,23,24], or both[22] based on the standard two-stage approach[23] or non-compartmental analyses[20–22,24,25], reporting on active or total ATG of different brands. The population approach, which we applied here, is considered superior over the standard two-stage approach and non-compartmental analysis[15–17,42]. Therefore, our results are not easily comparable to these results because of differences in methods.

With the developed pharmacokinetic model, active Thymoglobulin® exposure can be predicted in the entire pediatric age range. Dosing can be adjusted so that each child, irrespective of body weight and lymphocyte count, will have a predictable exposure. This is a major improvement when compared to the current dosing regimen, where exposure increases with body weight and/or decreasing baseline lymphocyte count, without evidence being available to support the rationale for this, and possibly even leading to significant side effects such as delayed or absent immune reconstitution. The next step in the development of an individual dosing regimen will be the determination of the therapeutic window.

Pharmacokinetic endpoints such as AUC can be related to clinical outcome measures as survival and the incidence of GvHD, rejection, relapse, and successful immune reconstitution, which have been shown to depend on ATG exposure[22,43,44]. These studies will result in an optimal active Thymoglobulin® exposure, which may vary based on transplant-related factors. The optimal exposure, combined with covariates influencing pharmacokinetics, will deter- mine the Thymoglobulin® dose for each individual patient.

Predictable exposure leads to predictable immune reconstitution, which is paramount for giving adjuvant cellular therapies for consolidation of the treatment for malignancies. Likewise, therapeutic decisions such as starting antivirals or tapering GvHD prophylaxis may also depend on immune reconstitution. All together, this is expected to result in an improvement of outcome after pediatric HCT.

CONCLUSION

We developed and evaluated a population pharmacokinetic model incorporating non-linear distribution and elimination, which accurately describes active Thymoglobulin® pharmacokinetics in the entire pediatric age range. Body weight and baseline lymphocytes were the most predictive covariates influencing the pharmacokinetics of active Thymoglobulin®, which could explain a major part of the inter-individual variability. The current dosing regimen is shown to be suboptimal, leading to varying exposures across age. Once the therapeutic window has been deter- mined, this model can be used to develop an individual dosing regimen for Thymoglobulin®, based on both body weight and lymphocyte counts. This individualized regimen may contribute to a better immune reconstitution, and thus outcome, of allogeneic HCT.

REFERENCES

1. Bacigalupo A, Lamparelli T, Bruzzi P, Guidi S, Alessandrino P, di Bartolomeo P, et al. Antithymocyte globulin for graft-versus-host disease prophylaxis in transplants from unrelated donors: 2 randomized studies from Gruppo Italiano Trapianti Midollo Osseo (GITMO). *Blood*. 2001; 98:2942–7.

2. Finke J, Bethge WA, Schmoor C, Ottinger HD, Stelljes M, Zander AR, et al. Standard graft-versus-host disease prophylaxis with or without anti-T-cell globulin in haematopoietic cell transplantation from matched unrelated donors: a randomised, open-label, multi- centre phase 3 trial. *Lancet Oncol*. 2009;10:855–64.

3. Byrne JL, Stainer C, Cull G, Haynes AP, Bessell EM, Hale G, et al. The effect of the serotherapy regimen used and the marrow cell dose received on rejection, graft-versus-host disease and outcome following unrelated donor bone marrow transplantation for leukaemia. *Bone Marrow Transpl*. 2000;25:411–7 .

4. Pihusch R, Holler E, Muhlbayer D, Gohring P, Stotzer O, Pihusch M, et al. The impact of antithymocyte globulin on short-term toxicity after allogeneic stem cell transplantation. *Bone Marrow Transpl*. 2002;30:347–54.

5. Theurich S, Fischmann H, Chemnitz J, Holtick U, Scheid C, Skoetz N. Polyclonal anti-thymocyte globulins for the prophylaxis of graft-versus-host disease after allogeneic stem cell or bone marrow transplantation in adults. *Cochrane Database Syst Rev*. 2012;9

6. Lindemans CA, Chiesa R, Amrolia PJ, Rao K, Nikolajeva O, de Wildt A, et al. Impact of thymoglobulin prior to pediatric unre- lated umbilical cord blood transplantation on immune reconstitution and clinical outcome. *Blood*. 2014;123:126–32.

7. Szabolcs P, Niedzwiecki D. Immune reconstitution after unrelated cord blood transplantation. *Cytotherapy*. 2007;9:111–22.

8. Jacobson CA, Turki A, McDonough S, Stevenson KE, Kim HT, Kao G, et al. Immune reconstitution after double umbilical cord blood stem cell transplantation: comparison with unrelated peripheral blood stem cell transplantation. *Biol Blood Marrow Transpl*. 2012;18:565–74.

9. Thomas-Vaslin V, Altes HK, De Boer RJ, Klatzmann D. Comprehensive assessment and mathematical modeling of T-cell population dynamics and homeostasis. *J Immunol*. 2008;180:2240–50.

10. Williams K, Hakim FT, Gress RE. T-cell immune reconstitution following lymphodepletion. *Semin Immunol*. 2008;19:318–30.

11. Krenger W, Blazar BR, Hollander GA. Thymic T-cell development in allogeneic stem cell transplantation. *Blood*. 2011;117:6768–76.

12. Bosch M, Dhadda M, Hoegh-Petersen M, Liu Y, Hagel LM, Podgorny P, et al. Immune reconstitution after anti-thymocyte globulin-conditioned hematopoietic cell transplantation. *Cytotherapy*. 2012;14:1258–75.

13. Chiesa R, Gilmour K, Qasim W, Adams S, Worth AJJ, Zhan H, et al. Omission of in vivo T-cell depletion promotes rapid expansion of naïve CD4+ cord blood lymphocytes and restores adaptive immunity within 2 months after unrelated cord blood transplant. *Br J Haematol*. 2012;156:656–66.

14. Kearns GL, Abdel-Rahman SM, Alander SW, Blowey DW, Leeder JS, Kauffman RE. Developmental pharmacology—drug disposition, action and therapy in infants and children. *N Engl J Med*. 2003;349:1157–67.

15. Admiraal R, van Kesteren C, Boelens JJ, Bredius RGM, Tibboel D, Knibbe CA. Towards evidence-based dosing regimens in children on the basis of population pharmacokinetic pharmacodynamic modelling. *Arch Dis Child*. 2014;99:267–72.

16. De Cock RFW, Piana C, Krekels EHJ, Danhof M, Allegaert K, Knibbe CA. The role of population PK-PD modelling in paediatric clinical research. *Eur J Clin Pharmacol*. 2011;67(Suppl 1):5–16.

17. Knibbe CAJ, Krekels EHJ, Danhof M. Advances in paediatric pharmacokinetics. *Expert Opin Drug Metab Toxicol*. 2011;7:1–8.

18. Bartelink IH, van Kesteren C, Boelens JJ, Egberts TCG, Bierings MB, Cuvelier GDE, et al. Predictive performance of a busulfan pharmacokinetic model in children and young adults. *Ther Drug Monit*. 2012;34:574–83.

19. Bartelink IH, van Reij EML, Gerhardt CE, van Maarseveen EM, de Wildt A, Versluys B, et al. Fludarabine and exposure-targeted busulfan compares favorably with busulfan/cyclophosphamide- based regimens in pediatric hematopoietic cell transplantation: maintaining efficacy with less toxicity. *Biol Blood Marrow Transpl*. 2013;20:1–9.

20. Waller EK, Langston AA, Lonial S, Cherry J, Somani J, Allen AJ, et al. Pharmacokinetics and pharmacodynamics of anti-thymocyte globulin in recipients of partially HLA-matched blood hematopoietic progenitor cell transplantation. *Biol Blood Marrow Transpl*. 2003;9:460–71.

21. Seidel MG, Fritsch G, Matthes-Martin S, Lawitschka A, Lion T, Po U, et al. Antithymocyte globulin pharmacokinetics in pediatric patients after hematopoietic stem cell transplantation. *J Pediatr Hematol Oncol*. 2005;27:532–6.

22. Remberger M, Persson M, Mattsson J, Gustafsson B, Uhlin M. Effects of different serum-levels of ATG after unrelated donor umbilical cord blood transplantation. *Transpl Immunol*. 2012;27:59–62.

23. Kakhniashvili I, Filicko J, Kraft WK, Flomenberg N. Heteroge- neous clearance of antithymocyte globulin after CD34+-selected allogeneic hematopoietic progenitor cell transplantation. *Biol Blood Marrow Transpl*. 2005;11:609–18.

24. Bashir Q, Munsell MF, Giralt S, de Padua Silva L, Sharma M, Couriel D, et al. Randomized phase II trial comparing two dose levels of thymoglobulin in patients undergoing unrelated donor hematopoietic cell transplant. *Leuk Lymphoma*. 2012;53:915–9.

25. Jol-van der Zijde C, Bredius R, Jansen-Hoogendijk A, Raaij- makers S, Egeler R, Lankester A, et al. IgG antibodies to ATG early after pediatric hematopoietic SCT increase the risk of acute GVHD. *Bone Marrow Transpl*. 2012;47:360–8.

26. Call SK, Kasow KA, Barfield R, Madden R, Leung W, Horwitz E, et al. Total and active rabbit antithymocyte globulin (rATG;Thymoglobulin) pharmacokinetics in pediatric patients undergoing unrelated donor bone marrow transplantation. *Biol Blood Marrow Transpl*. 2009;15:274–8.

27. Regan JF, Lyonnais C, Campbell K, Van Smith L. Total and active thymoglobulin levels: effects of dose and sensitization on serum concentrations. *Transpl Immunol*. 2001;9:29–36.

28. Rebello P, Hale G. Pharmacokinetics of CAMPATH-1H: assay development and validation. *J Immunol Methods*. 2002;260: 285–302.

29. Bauer RJ. NONMEM users guide: introduction to NONMEM 7.2.0. Ellicott City: ICON Development Solutions; 2011. p. 1–131.

30. Keizer RJ, van Benten M, Beijnen JH, Schellens JHM, Huitema ADR. Pirana and PCluster: a modeling environment and cluster infrastructure for NONMEM. *Comput Methods Progr Biomed*. 2011;101:72–9.

31. R Core Team. R: a language and environment for statistical computing. Vienna: R Foundation for Statistical Computing; 2008.

32. Beal SL. Ways to fit a PK model with some data below the quantification limit. *J Pharmacokinet Pharmacodyn*. 2001;28: 481–504.

33. Krekels EHJ, Neely M, Panoilia E, Tibboel D, Capparelli E, Danhof M, et al. From pediatric covariate model to semiphysiological function for maturation: part I-extrapolation of a covariate model from morphine to Zidovudine. *CPT Pharmacometrics Syst Pharmacol.* 2012;1:e9.

34. Krekels EHJ, Johnson TN, den Hoedt SM, Rostami-Hodjegan A, Danhof M, Tibboel D, et al. From pediatric covariate model to semiphysiological function for maturation: part II-sensitivity to physiological and physicochemical properties. *CPT Pharmacometrics Syst Pharmacol.* 2012;1:e10.

35. Krekels EHJ, van Hasselt JGC, Tibboel D, Danhof M, Knibbe CA. Systematic evaluation of the descriptive and predictive performance of paediatric morphine population models. *Pharm Res.* 2011;28:797–811.

36. Lindbom L, Pihlgren P, Jonsson EN, Jonsson N. PsN-Toolkit–a collection of computer intensive statistical methods for non-linear mixed effect modeling using NONMEM. *Comput Methods Progr Biomed.* 2005;79:241–57.

37. Comets E, Brendel K, Mentre ́ F. Computing normalised prediction distribution errors to evaluate nonlinear mixed-effect mod- els: the npde add-on package for R. *Comput Methods Progr Biomed.* 2008;90:154–66.

38. Gibiansky L, Gibiansky E, Kakkar T, Ma P. Approximations of the target-mediated drug disposition model and identifiability of model parameters. *J Pharmacokinet Pharmacodyn.* 2008;35: 573–91.

39. Yan X, Mager DE, Krzyzanski W. Selection between Michaelis- Menten and target-mediated drug disposition pharmacokinetic models. *J Pharmacokinet Pharmacodyn.* 2010;37:25–47.

40. Mould DR, Baumann A, Kuhlmann J, Keating MJ, Weitman S, Hillmen P, et al. Population pharmacokinetics-pharmacody- namics of alemtuzumab (Campath) in patients with chronic lymphocytic leukaemia and its link to treatment response. *Br J Clin Pharmacol.* 2007;64:278–91.

41. Feng X, Scheinberg P, Biancotto A, Rios O, Donaldson S, Wu C, et al. In vivo effects of horse and rabbit antithymocyte globulin in patients with severe aplastic anemia. *Haematologica.* 2014; 99:1433–40

42. Knibbe CAJ, Danhof M. Individualized dosing regimens in children based on population PKPD modelling: are we ready for it? *Int J Pharm.* 2011;415:9–14.

43. Remberger M, Svahn B, Mattsson J, Ringden O. Dose study of thymoglobulin during conditioning for unrelated donor allogeneic stem-cell transplantation. *Transplantation.* 2004;78:122–7.

44. Remberger M, Ringden O, Hagglund H, Svahn B-M, Ljungman P, Uhlin M, et al. A high antithymocyte globulin dose increases the risk of relapse after reduced intensity conditioning HSCT with unrelated donors. *Clin Transpl.* 2013;27:E368–74.
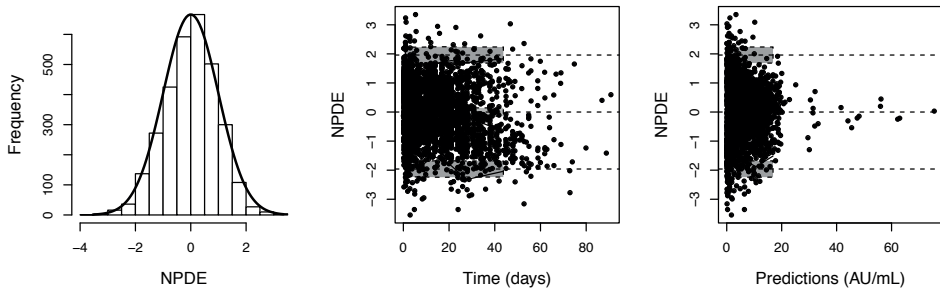
SUPPLEMENTALS

Figure S1. Normalized prediction distribution of errors (NPDE). Panel a: histogram of the NPDE with the solid line representing a normal distribution with a mean of 0 and variance of 1. Panel b: NPDE versus observations, panel c: NPDE versus predictions. Grey blocks: 95% confidence interval of NPDE.